

Control of atomic currents using a quantum stirring device

MORITZ HILLER^{1,2,3}, TSAMPIKOS KOTTOS^{1,2} and DORON COHEN⁴

¹ Department of Physics, Wesleyan University, Middletown, Connecticut 06459, USA

² MPI for Dynamics and Self-Organization, Bunsenstr. 10, D-37073 Göttingen, Germany

³ Physikalisches Institut, Albert-Ludwigs-Universität, Hermann-Herder-Str. 3, D-79104 Freiburg, Germany

⁴ Department of Physics, Ben-Gurion University, Beer-Sheva 84105, Israel

PACS 03.65.-w – Quantum mechanics.

PACS 03.65.Vf – Phases: geometric; dynamic or topological.

PACS 05.30.Jp – Boson systems.

Abstract. - We propose a BEC stirring device which can be regarded as the incorporation of a quantum pump into a closed circuit: it produces a DC circulating current in response to a cyclic adiabatic change of two control parameters of an optical trap. We demonstrate the feasibility of this concept and point out that such device can be utilized in order to probe the interatomic interactions.

The realization of Bose-Einstein Condensation (BEC) of ultra-cold atoms in optical lattices and atom chips [1] and the availability of conveyor belts [2] is considered to be a major breakthrough with potential applications in the arena of quantum information processing [3], atom interferometry [4–6], lasers [1, 7] and atom diodes and transistors [8–10]. A major advantage of BEC based devices, as compared to conventional solid-state structures, lies in the extraordinary degree of precision and control that is available, regarding not only the confining potential, but also the strength of the interatomic interactions, their preparation and the measurement of the atomic cloud. Accordingly it is envisioned that the emerging field of “atomtronics” will provide a new generation of nanoscale devices.

The possibility to induce DC currents by periodic (AC) modulation of the potential is familiar from the context of electronic devices. If an open geometry is concerned, it is known as “quantum pumping” [11], while for closed geometries we use the term “quantum stirring” [12]. We consider below the stirring of condensed ultra-cold atoms due to the periodic variation of the on-site potentials and of the tunneling rates between adjunct confining traps. We show that the nature of the transport process depends crucially on the sign and on the strength of the interatomic interactions. We distinguish between four regimes of dynamical behavior: For strong repulsive interaction the particles are transported one-by-one, which we call *sequential crossing*; for weaker repulsive interaction we observe either *gradual crossing* or coherent

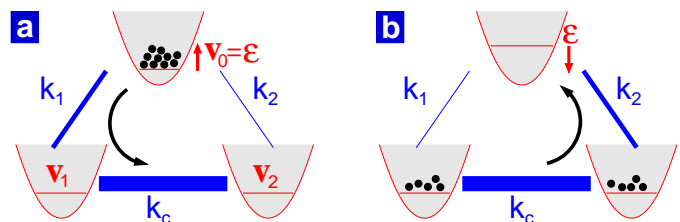


Fig. 1: (Color online) **Illustration of the model system.** In the first half of the cycle **a** the particles are transported from the gated-well to the double-well via the k_1 bond, while in the second half of the cycle **b** the particles are transported back from the double-well to the gated-well via the k_2 bond. See the text for further details.

mega crossing; finally, for strong attractive interaction the particles move together as one composite unit from trap to trap.

Model – The simplest model that captures the physics of quantum stirring is the three-site Bose-Hubbard Hamiltonian (BHH) [10, 13–15] (see Fig. 1)¹. We call the $i=0$ site “gated-well” since we later assume that we have control over its potential energy $v_0 = \epsilon$. The $i=1,2$ sites form

¹ The three-site BHH is a prototype system for many recent studies [13]. A classical analysis of this system was performed in [15] where it was shown that for appropriate system parameters and initial conditions chaotic dynamics would emerge. In this work we consider adiabatic driving of ground state preparation and therefore chaotic motion is not an issue.

a two level “double-well” with potential energy $v_1=v_2=0$. The N boson BHH is:

$$\hat{\mathcal{H}} = \sum_{i=0}^2 \left[v_i \hat{n}_i + \frac{U}{2} \hat{n}_i (\hat{n}_i - 1) \right] - k_c \hat{b}_2^\dagger \hat{b}_1 - \sum_{i=1,2} k_i \hat{b}_i^\dagger \hat{b}_0 + \text{h.c.} \quad (1)$$

We set $\hbar=1$ which corresponds to measuring energies in units of frequency. Furthermore, without loss of generality we choose time units such that $k_c=1$. Accordingly the two single particle levels of the double-well are $\varepsilon_{\pm} = \pm 1$. The annihilation and creation operators \hat{b}_i and \hat{b}_i^\dagger obey the canonical commutation relations $[\hat{b}_i, \hat{b}_j^\dagger] = \delta_{i,j}$ while the operators $\hat{n}_i = \hat{b}_i^\dagger \hat{b}_i$ count the number of bosons at site i . The interaction strength between two atoms in a single site is given by $U = 4\pi a_s V_{\text{eff}}/\mathbf{m}$ where V_{eff} is the effective volume, \mathbf{m} is the atomic mass, and a_s is the s -wave scattering length which can be changed by applying an additional magnetic field [16]. The on-site potentials v_i as well as the coupling strengths k_i are controlled by changing the confining potential. The main assumption underlying the BHH is that the single-particle ground state wavefunctions are sufficiently localized at the sites, and that for the temperatures involved they are well separated in energy from the excited single-particle levels. Experimentally, such deep trapping potentials can accommodate several hundred particles [17].

The couplings between the gated-well and the two ends of the double-well are k_1 and k_2 . We assume that both are much smaller than k_c (for the two-mode BEC dynamics see for example [18]). It is convenient to define the two control parameters of the pumping as $X_1 = (1/k_2) - (1/k_1)$ and $X_2 = \varepsilon$. By periodic cycling of the parameters (X_1, X_2) we can obtain a non-zero amount (Q) of transported atoms per cycle. The pumping cycle is illustrated in Figs. 1,2. Initially all the particles are located in the gated-well which has a sufficiently negative on-site potential energy ($X_2 < 0$). In the first half of the cycle the coupling is biased in favor of the k_1 route ($X_1 > 0$) while X_2 is raised until (say) the gated-well is empty². In the second half of the cycle the coupling is biased in favor of the k_2 route ($X_1 < 0$), while X_2 is lowered until the gated-well is full. Assuming $U=0$, the gated-well is depopulated via the k_1 route into the lower energy level ε_- during the first half of the cycle, and re-populated via the k_2 route during the second half of the cycle. Accordingly the net effect is to have a non-zero Q . If we had a single particle in the system, the net effect would be to pump roughly one particle per cycle. If we have N non-interacting particles, the result of the same cycle is to pump roughly N particles per cycle³. We would like to know what is the actual

²Later we estimate the required X_2 variation in order to have all the particles transferred from the gated-well to the double well. We also analyze smaller pumping cycles (see Fig. 3b) for which only a fraction of particles gets through.

³Through the driving cycle the total number of bosons remains constant. The energy is not a constant of motion, but in the adia-

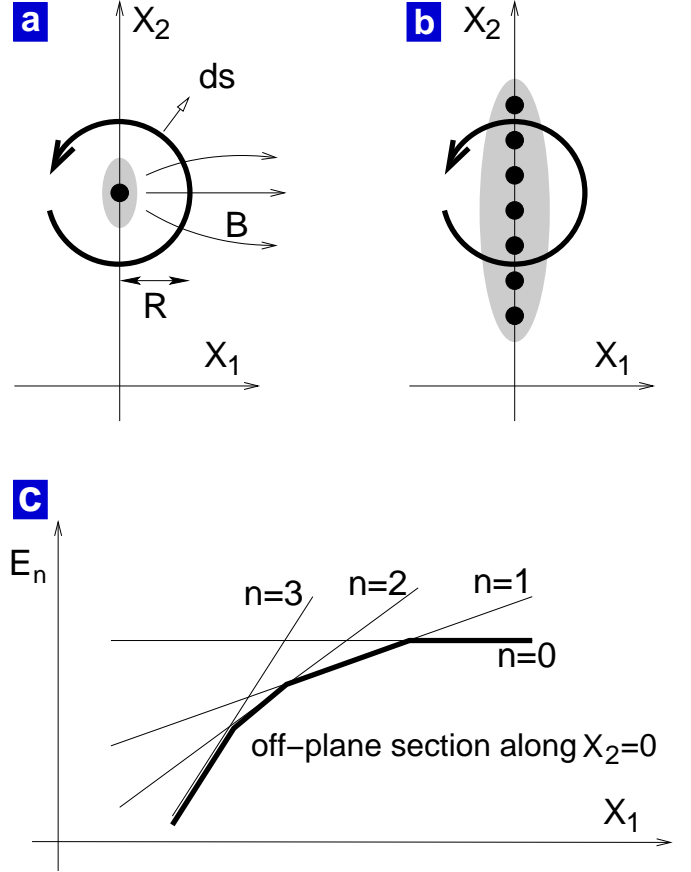


Fig. 2: **Illustration of the pumping cycle.** See the text for further details. For a large cycle that encircles the whole shaded region we have $Q \approx N$. Position of the monopoles: **a** no interactions, **b** with interactions. **c**, the energy levels along the $X_1 = 0$ axis are schematically plotted for an $N = 3$ system.

result using a proper quantum mechanical calculation, and furthermore we would like to investigate what is the effect of the interatomic interaction U on the result.

Methods – Within the framework of linear response theory the induced current is $I = -G_1 \dot{X}_1$ if we change X_1 and $I = -G_2 \dot{X}_2$ if we change X_2 . The coefficients G_1 and G_2 in these linear relations are *defined* as the elements of the geometric conductance matrix, and can be calculated using the Kubo formula approach (see below). Integrating the current over a full cycle we get

$$Q = \oint_{\text{cycle}} I dt = - \oint (G_1 dX_1 + G_2 dX_2). \quad (2)$$

In order to calculate the geometric conductance we use the Kubo formula approach to quantum pumping [19] which is based on the theory of adiabatic processes [20]. It turns out that in the strict adiabatic limit G is related to the vector field \mathbf{B} in the theory of the Berry phase which is

in the adiabatic limit the system comes back to the same state at the end of each cycle.

known as the ‘‘Berry Curvature’’. The adiabatic slowness condition on \dot{X} in the present context, taking into account the two-orbital approximation, is discussed in Section 4 of [21]. Using the notations $\mathbf{B}_1 = -G_2$ and $\mathbf{B}_2 = G_1$ it is illuminating to rewrite Eq.(2) as

$$Q = \oint \mathbf{B} \cdot d\vec{s}, \quad (3)$$

where we define the normal vector $d\vec{s} = (dX_2, -dX_1)$ as illustrated in Fig. 2. The calculation of the so-called Kubo-Berry Curvature is done using the following formula [19]:

$$\mathbf{B}_j = \sum_{n \neq n_0} \frac{2 \operatorname{Im}[\mathcal{I}_{n_0 n}] \mathcal{F}_{nn_0}^j}{(E_n - E_{n_0})^2}. \quad (4)$$

Above $\mathcal{I} = i/2 [k_1(\hat{b}_0^\dagger \hat{b}_1 - \hat{b}_1^\dagger \hat{b}_0) + k_2(\hat{b}_2^\dagger \hat{b}_0 - \hat{b}_0^\dagger \hat{b}_2)]$ is the averaged current⁴ via the bonds $0 \rightarrow 1$ and $2 \rightarrow 0$, while $\mathcal{F}^j = -\partial \mathcal{H} / \partial X_j$ is the generalized force associated with the control parameter X_j . The index n labels the eigenstates of the many-body Hamiltonian. We assume from now on that n_0 is the BEC ground state¹.

The advantage of the above, so called ‘‘geometric’’ point of view is in the intuition that it gives for the result: Formally the field \mathbf{B} is like a projection of a fictitious magnetic field in an embedding three-dimensional X space (the third coordinate X_3 is formally defined such that $\mathcal{I} = -\partial \mathcal{H} / \partial X_3$). The flux of this fictitious magnetic field through any out-of-plane surface which is enclosed by the pumping cycle gives the so-called Berry phase, while the line integral over this fictitious magnetic field, i.e. Eq.(3)⁵, gives Q . As implied by inspection of Eq.(4) the sources of \mathbf{B} are located at points where the ground level n_0 has a degeneracy with the next level. A simple argument implies that this ‘‘magnetic charge’’ is quantized like Dirac monopoles, else the Berry phase would be ill-defined. For details see [19]. In our model system for $U=0$ all the ‘‘magnetic charge’’ is concentrated in one point. As the interaction U becomes larger the $(N+1)$ -fold degeneracy of the levels is lifted, and this ‘‘magnetic charge’’ disintegrates into N elementary ‘‘monopoles’’ (see Fig. 2). We further discuss the energy spectrum in the next section.

Regimes – We define the average coupling as $\kappa = (k_1 + k_2) / \sqrt{2}$. In the zeroth-order approximation k_1 and k_2 are neglected, and later we take them into account as a perturbation. For $\kappa=0$ the number (n) of particles in the gated-well becomes a good quantum number hence we can associate the level index n with the number of particles

⁴Due to the continuity equation the same result for Q is obtained irrespective of whether we measure the current via the $0 \rightarrow 1$ bond or via the $2 \rightarrow 0$ bond. The advantage of using the ‘‘symmetrized’’ version for \mathcal{I} is that the same amount of particles is being transported during both halves of the cycle, allowing us to focus on (say) the first half and then double the result.

⁵In the $X_3=0$ plane the third component of the fictitious magnetic field is zero due to the time-reversal symmetry [19].

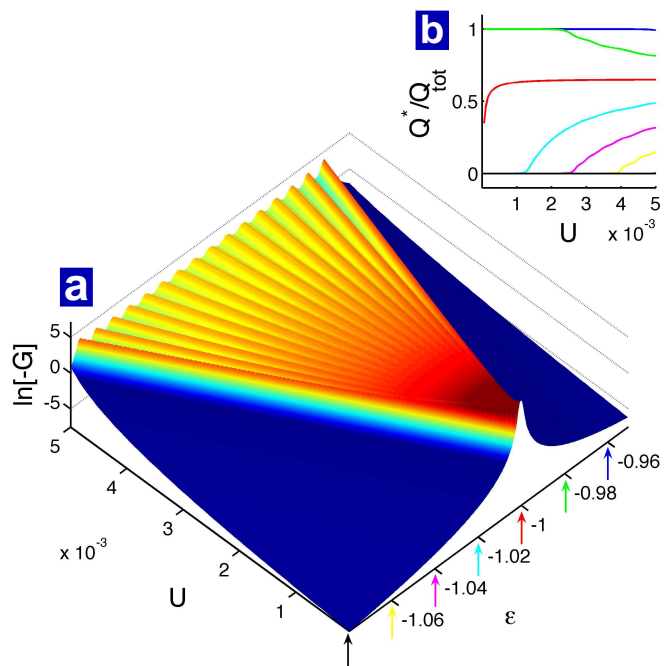


Fig. 3: (Color online) **Conductance during the first half of the pumping cycle.** **a**, the conductance G_2 as a function of the on-site potential ε , for various values of U . In the numerical simulations (see also Fig. 4) we are using exact diagonalization of the trimer Hamiltonian (1). For the evaluation of G we use Eq. (2) while for Q we use Eq. (4). The other parameters are $N = 16$ particles, $\kappa = 0.0003/\sqrt{2}$ and $(k_1 - k_2)/\sqrt{2} = 0.0001/\sqrt{2}$. As the interaction U becomes larger one observes the crossover from a single to individual peaks in the conductance. **b**, the U -dependence of the integrated charge Q^* , calculated for wide rectangular cycles for which X_2 is varied within $[-\infty, \varepsilon^*]$. The values of ε^* are indicated by arrows of the same color in the main panel.

in the gated-well. Furthermore, we adopt a ‘‘two-orbital approximation’’: we assume that there is non-zero occupation only in the gated-well and in the lower double-well level, which is valid if $NU \ll k_c$. Note also that we assume an adiabatic process³, and accordingly non-adiabatic transitions to the higher orbitals can be safely neglected [21].

Within the two-orbital approximation the many body energies are $E_n = E_{\text{gated-well}}(n) + E_{\text{double-well}}(N-n)$, where $n=0, 1, \dots, N$, and $E_{\text{gated-well}}(n) = \varepsilon n + (1/2)U(n-1)n$, and $E_{\text{double-well}}(N-n) = -(N-n) + (1/4)U(N-n-1)(N-n)$. The location $\varepsilon_n = -1 + \frac{1}{2}U \times (N-3n+2)$ of the $n \mapsto (n-1)$ crossing is determined from the degeneracy condition $E_n - E_{n-1} = 0$, where $n=1, 2, \dots, N$. The N crossings are distributed within $\varepsilon \in -1 + (N-1)[-U, U/2]$. The rescaled version of the control variable is $\hat{\varepsilon} = (\varepsilon+1)/((N-1)U)$, and its support is $-1 < \hat{\varepsilon} < 1/2$. The distance between the crossings, while varying the gated-well potential ε , is U . Once we take κ into account we get *avoided* crossings of width $\delta\varepsilon_n = [(N+1-n)n/2]^{1/2}\kappa$. If κ/UN is large these avoided

crossings merge and eventually we get one mega crossing.

For the purpose of further analysis we apply the two-orbital approximation, within which the many body Hamiltonian matrix is $\mathcal{H}_{nm} = E_n \delta_{n,m} - \kappa_n \delta_{n,n\pm 1}$, where $n=0, \dots, N$ and the couplings are defined as $\kappa_n = \langle n-1 | \mathcal{H} | n \rangle$. The calculation involves the matrix elements of $b_i^\dagger b_0$, leading to $\kappa_n = [(N+1-n)n]^{1/2} \kappa$. Analogous expression applies to the current operator where κ is replaced by $(k_1 - k_2)/\sqrt{2}$. For large U , as ε is varied, we encounter (say for $N=3$) a sequence of distinct Landau-Zener transitions ($|3\rangle \mapsto |2\rangle \mapsto |1\rangle \mapsto |0\rangle$). The distance between avoided crossings is of order U while their width is $\delta\varepsilon_n = \kappa_n$. The widest crossings are at the center with $\delta\varepsilon_n \sim N\kappa$. This should be contrasted with the energy scales U and NU that describe the span of the crossings. Accordingly we deduce that for repulsive interaction there are three distinct regimes: for $U \ll \kappa/N$ we have a ‘‘mega crossing’’; for $U \gg N\kappa$ we have the ‘‘sequential crossing regime’’, while in the intermediate regime we have a ‘‘gradual crossing’’. Below we summarize the results in the various regimes. In particular Eq.(7) is obtained from Eq.(4) with a two level approximation for each crossing. We also related briefly to the $U < 0$ regime.

Results – Most of the contribution to the line integral in Eq.(2) comes as we change X_2 during the avoided crossings that have been discussed in the previous section. If we close the pumping cycle outside of this limited range, then the X_1 -variation can be safely neglected. Accordingly we refer from now on to $G_2 = G$ only. An overview of the numerical results for the conductance is shown in Fig. 3, where we plot G as a function of X_2 for various interaction strengths U . In the same figure we report the normalized amount of particles Q for various driving cycles. As the shape of G_2 changes, the dependence of Q on the X_2 -span of the pumping cycle becomes of importance. Thus, by measuring Q we obtain information on the strength of the interatomic interactions.

In Fig. 4 more details are presented: besides G we also plot the X_2 -dependence of the energy levels, and of the site population. Four representative values of U are considered including also the $U < 0$ case. Let us discuss the observed results. For $U=0$ all the particles cross ‘‘together’’ from the gated-well orbital to the ε_- double-well orbital. We call this type of dynamics ‘‘mega crossing’’. The outcome is just N times the single particle result:

$$G = -N \frac{(k_1^2 - k_2^2)/2}{[(\varepsilon - \varepsilon_-)^2 + 2(k_1 + k_2)^2]^{3/2}}, \quad (5)$$

which can be expressed in terms of the control parameters (X_1, X_2). This result approximately hold as long as $U \ll \kappa/N$. Integrating over a full cycle one obtains

$$Q = N \frac{[1 + (\kappa R)^2]^{1/2} - 1}{\kappa R}, \quad (6)$$

where R is the radius of the pumping cycle (see Fig. 2). For small cycles we get $Q \approx N\kappa R/2$, while for large cycles

we get the limiting value $Q \approx N$. In the other extreme, for very repulsive interaction ($U \gg N\kappa$) we get

$$G = - \left(\frac{k_1 - k_2}{k_1 + k_2} \right) \sum_{n=1}^N \frac{(\delta\varepsilon_n)^2}{[(\varepsilon - \varepsilon_n)^2 + (2\delta\varepsilon_n)^2]^{3/2}}. \quad (7)$$

For intermediate values $U \in [\kappa/N, N\kappa]$, we find neither the sequential crossing of Eq.(7), nor the mega-crossing of Eq.(5), but rather a gradual crossing. Namely, in this regime, over a range $\Delta X_2 = (3/2)(N-1)U$ we get a constant geometric conductance:

$$G \approx - \left[\frac{k_1 - k_2}{k_1 + k_2} \right] \frac{1}{3U} \quad (8)$$

which reflects in a simple way the interaction strength. This formula was deduced by extrapolating Eq.7, and then was validated numerically (lower panel of Fig. 4c).

As discussed above for large positive U the $(N+1)$ -fold ‘‘degeneracy’’ of the $U=0$ Landau-Zener crossing is lifted, and we get a sequence of N Landau-Zener crossings (for schematic illustration see the lower panel of Fig. 2, and compare with the numerical results in the upper panels of Fig. 4). Also for $U < 0$ this $(N+1)$ -fold ‘‘degeneracy’’ is lifted, but in a different way: the levels separate in the ‘‘vertical’’ (energy) direction rather than ‘‘horizontally’’ (see upper panels of Fig. 4). Accordingly all the particles execute a single two-level transition from the gated-well to the double-well (see Fig. 4a). This direct Landau-Zener transition from the $n=N$ level to the $n=0$ level is very sharp because it is mediated by an N -th order virtual transition via the intermediate n states. Accordingly, for sufficiently strong attractive interaction all the particles move together from the gated-well to *one* of the double-well sites. When the sign of X_1 is reversed they are transported from one end of the double-well to the other end (not shown). This should be clearly distinguished from the $(N+1)$ -fold degenerated transition to the lower double-well *level* which is observed in the $U=0$ case.

Summary – The theoretical [10,18,22] and experimental [23] study of driven dynamics in single and double site systems is the state of the art. Study of three-site systems adds the exciting topological aspect: controlled atomic current can be induced using optical lattice technology [24]. The actual measurement of induced neutral currents poses a challenge to experimentalists. In fact there is a variety of techniques that have been proposed for this purpose. For example one can exploit the Doppler effect in the perpendicular direction, which is known as the rotational frequency shift [25]. The analysis of the prototype trimer system reveals the crucial importance of interactions. The interactions are not merely a perturbation: rather they determine the nature of the transport process. We expect the induced circulating atomic current to be extremely accurate, which would open the way to various applications, either as a new metrological standard, or as

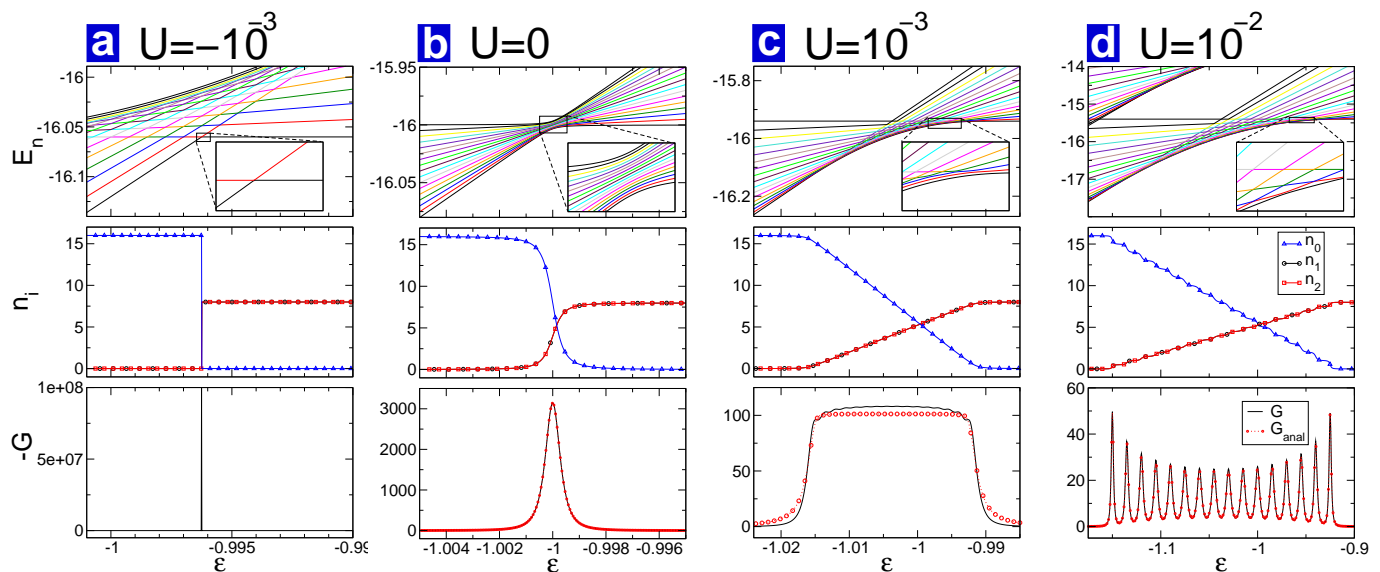


Fig. 4: (Color online) **Evolution of the energy levels, the site occupation and the conductance.** Further details relating to the data of Fig. 3. We refer to four representative values of U , which are indicated on top of each set of panels. *Upper panels:* the lowest $N+1$ energy levels E_n which dominate the conductance G_2 are plotted as a function of $X_2 = \varepsilon$. The insets represent magnifications of the indicated areas. *Middle panels:* the site occupations n_0 (blue \triangle), n_1 (black \circ), n_2 (red \square). *Lower panels:* the corresponding conductance G_2 as a function of ε . Numerical results are represented by solid black lines while the dotted red line corresponds to the analytical result (5) in **b** and to (7) in **c, d**.

a component of a new type of quantum information or processing device.

This research was supported by a grant from the United States-Israel Binational Science Foundation (BSF) and the DFG (Forschergruppe 760).

REFERENCES

- [1] B.P. Anderson et al., Science **282**, 1686 (1998). D. Jaksch et al., Phys. Rev. Lett. **81**, 3108 (1998). C. Orzel et al., Science **291**, 2386 (2001). M. Greiner et al., Nature **415**, 39 (2002). I. Bloch, Nature Phys. **1**, 23-30 (2005) R. Folman et al., Phys. Rev. Lett. **84**, 4749 (2000).
- [2] W. Hansel, et al., Nature **413**, 498 (2001); W. Hansel, et al., New J. Phys. **7**, 3 (2005).
- [3] J. Schmiedmayer, R. Folman, T. Calarco, J. Mod. Opt. **49**, 1375 (2002).
- [4] T. Schumm, et al., Nat. Phys. **1**, **57** (2005).
- [5] Y-J Wang, et al., Phys. Rev. Lett. **94**, 090405 (2005); E. Andersson, et al., Phys. Rev. Lett. **88**, 100401 (2002).
- [6] M. R. Andrews, et al., Science **275**, 637 (1997).
- [7] M. O. Mewes, et al., Phys. Rev. Lett. **78**, 582 (1997); E. W. Hagley, et al., Science **283**, 1706 (1999); Y. Shin, et al., Phys. Rev. Lett. **92**, 050405 (2004).
- [8] A. Micheli, et al., Phys. Rev. Lett. **93**, 140408 (2004).
- [9] B. T. Seaman, et al., (2006) [cond-mat/0606625].
- [10] J. A. Stickney, D. Z. Anderson, A. A. Zozulya, Phys. Rev. A **75**, 013608 (2007).
- [11] D. J. Thouless, Phys. Rev. B **27** 6083 (1983). Q. Niu and D. J. Thouless, J. Phys. A **17** 2453 (1984). M. Buttiker, H. Thomas and A Pretre, Z. Phys. B-Condens. Mat., **94**, 133-137 (1994). P. W. Brouwer, Phys. Rev. B **58**, R10135 (1998). B. L. Altshuler, L. I. Glazman, Science **283**, 1864 (1999). M. Switkes, et al., Science **283**, 1905 (1999).
- [12] G. Rosenberg and D. Cohen, J. Phys. A **39**, 2287 (2006), and further references therein.
- [13] M. Hiller, T. Kottos, and T. Geisel, Phys. Rev. A **73**, 061604(R) (2006), and further references therein.
- [14] J. D. Bodyfelt, M. Hiller, and T. Kottos, Europhys. Lett. **78**, 50003 (2007).
- [15] R. Franzosi, V. Penna, Phys. Rev. E **67**, 046227 (2003); K. Nemoto, et al., Phys. Rev. A **63**, 013604 (2000).
- [16] A. J. Legget, Rev. Mod. Phys. **73**, 307 (2001).
- [17] G. J. Milburn, J. Corney, E. M. Wright, and F. D. Walls, Phys. Rev. A. **55**, 4318 (1997).
- [18] M. Jääskeläinen, P. Meystre, Phys. Rev A **73**, 013602 (2006); D. R. Dounas-Frazer, L. D. Carr, quant-ph/0610166 (2006); K. W. Mahmud, H. Perry, W. P. Reinhardt, J. Phys. B **36**, L265 (2003); M. Albiez et al., Phys. Rev. Lett. **95**, 010402 (2005).
- [19] D. Cohen, Phys. Rev. B **68**, 155303 (2003).
- [20] M.V. Berry, Proc. R. Soc. Lond. A **392**, 45 (1984). J.E. Avron, A. Raveh and B. Zur, Rev. Mod. Phys. **60**, 873 (1988). M.V. Berry and J.M. Robbins, Proc. R. Soc. Lond. A **442**, 659 (1993).
- [21] M. Chuchem and D. Cohen, J. Phys. A **41**, 075302 (2008).
- [22] B. Wu and J. Liu, Phys. Rev. Lett. **96**, 020405 (2006); J. Liu, B. Wu, Q. Niu, Phys. Rev. Lett. **90**, 170404 (2003).
- [23] C.-S. Chuu, et. al, Phys. Rev. Lett. **95**, 260403 (2005); A. M. Dudarev, M. G. Raizen, and Q. Niu, Phys. Rev. Lett. **98**, 063001 (2007).
- [24] L. Amico, A. Osterloh, F. Cataliotti, Phys. Rev. Lett. **95**, 063201 (2005).
- [25] I. Bialynicki-Birula and Z. Bialynicka-Birula, Phys. Rev. Lett. **78**, 2539 (1997).